

## Highly Sensitive Determination of Hg(II) Using Self-Assembled Monolayer of 4-Pyridineethanthiol on Gold Nanoparticles Modified-Glassy Carbon Electrode Pretreated by Exclusively Cathodic Polarization

P.H. PHONG<sup>1,\*</sup>, N.H. ANH<sup>1</sup>, L.Q. HUNG<sup>1</sup>, N.T.C. HA<sup>2</sup> and V.T.T. HA<sup>1</sup>

<sup>1</sup>Institute of Chemistry, Vietnam Academy of Science and Technology, 18 Hoang Quoc Viet Road, Cau Giay District, Hanoi, Vietnam

<sup>2</sup>Faculty of Chemistry, Hanoi University of Science, Vietnam National University, 19 Le Thanh Tong Street, Hanoi, Vietnam

\*Corresponding author: Fax: +84 4 8361283; Tel: +84 4 38362008; E-mail: phongph@ich.vast.ac.vn

(Received: 11 August 2012;

Accepted: 20 May 2013)

AJC-13522

Modification of the glassy carbon electrode (GCE) with gold nanoparticles coated by 4-pyridineethanthiolate hydrochloride self-assembled monolayer for determination of Hg<sup>2+</sup> by differential pulse voltammetry has been studied. Use of the exclusively cathodic polarization method at potential of -1.0 V to activate the GCE surface enhanced the sensitivity of the analysis compared with use of both anodic and cathodic polarizations or exclusive anodic polarization. The calibration curve for the differential pulse voltammetry peak current of Hg<sup>2+</sup> versus its concentration showed two linear regions. The first region demonstrated linearity in the range from  $5.0 \times 10^{-11}$  to  $5.0 \times 10^{-9}$  M with a correlation coefficient of 0.993. The slope of the second linear region was smaller than the first region's slope with the linear range of  $5.0 \times 10^{-9}$ - $7.0 \times 10^{-7}$  M ( $R^2 = 0.998$ ). The detection limit was  $4.5 \times 10^{-12}$  M estimated from three times the standard deviation of the background noise. The selectivity of the modified GCE for Hg<sup>2+</sup> over other metals ions in aqueous solutions was remarkably high (at least 100-fold excess). The applicability of the modified GCE in determination of Hg<sup>2+</sup> in real water samples without any pretreatment was successfully demonstrated.

**Key Words:** Exclusively cathodic polarization, 4-Pyridineethanthiol hydrochloride, Self-assembled monolayer, Gold nanoparticles.

### INTRODUCTION

All forms of mercury are recognized to be a cause of a variety of health effects, including neurological, renal, respiratory, immune, dermatologic, reproductive and developmental sequelae<sup>1</sup>. In fact mercury is usually present at low concentrations in environmental samples as free ions, complexed with inorganic and organic ligands or as organomercury compounds<sup>2</sup>. Since mercury can be toxic even at low concentration the determination of this element in environmental samples calls for highly sensitive, selective and portable devices with simple procedures that can be used either in laboratory or for on-site measurements. Among them, the use of modified working electrodes in electrochemical method has received particular attention due to their advantages which include the broad range of electrode materials. Further, measurement methodologies in this method overcome expensive and sophisticated instrumentation<sup>3-7</sup>. Many modifications have been studied for different electrode materials. For example, glassy carbon/graphite electrode is modified with gold nanoparticles<sup>8-11</sup>, glassy carbon/carbon paste electrode is functionalized with ligands able to complex Hg<sup>2+</sup><sup>12-15</sup>, with polymer<sup>16</sup> or gold/

carbon paste electrode modified with protein<sup>17,18</sup> for voltammetric determination. Additionally, modification of solid gold electrode with a self-assembled monolayer (SAM) based on the strong affinity between gold and sulfur atom has been attractive to many studies<sup>19-24</sup>. The results indicate a marked improvement in selectivity and sensitivity of the analysis when using SAM-modified electrodes. However, the main drawback of the use of solid gold substrates for formation of SAMs are their high cost and the need to carefully polish the electrode surface to achieve reproducibility. Thus, a gold film on GCE is a good alternative because it is low cost than the bulk electrodes, renewable surface as well as it can form stable and highly reproducible film. Such modified GCE thus provides significantly improved performance in Hg<sup>2+</sup> determination compared to unmodified GCE and bare gold electrode<sup>25</sup>. In addition, the advantage of gold nanoparticles (Au-NPs) film over the bulk gold electrodes is to significantly increase the microscopic area, leading to an increase in interactions between SAM on Au-NPs and Hg<sup>2+</sup> ions in the bulk solution.

In order to increase the repeatability of the electrochemical results various methods have been used for activating

the surface, such as mechanical polishing<sup>24</sup>, ultrasonic cleaning<sup>25</sup>, vacuum heating activation<sup>26,27</sup>. Furthermore, the rate of the electron transfer steps at the electrode surface can also be improved by adding electrochemical steps to the physical pretreatment<sup>28,29</sup>. While methods like application of potential cycling between two preset potentials<sup>8,30-33</sup>, static polarization at anodic or cathodic potential followed by potential sweeping in a wide range<sup>8,11,34</sup>, static polarization at anodic potential followed by static polarization at cathodic potential<sup>15</sup> have been reported as prominent method for GCE activation used for determination of Hg<sup>2+</sup>, no study focus on the role of the exclusive precathodisation as a pretreatment method in analysis of this heavy metal ion.

In the present paper, we report the use of the exclusively cathodic polarization in the pretreatment of GCE to modify with gold nanoparticles coated by 4-pyridineethanthiolate hydrochloride self-assembled monolayer (PET-SAM) applied in selective determination of Hg<sup>2+</sup>. We show the advantage of this pretreatment method in enhancing the sensitivity of the analysis compared with the use of cathodic and/or anodic polarizations. We wish to signify that this preliminary work emphasizes the potential of the PET-SAM on gold nanoparticles as a versatile tool to modify the GCE for analysis of Hg<sup>2+</sup> at ultratrace concentrations.

## EXPERIMENTAL

4-Pyridineethanthiol hydrochloride (PET) purchased from Wako Chemicals was used without further purification. Hg(NO<sub>3</sub>)<sub>2</sub> stock solution (5.0 × 10<sup>-3</sup> M) purchased from Merck was used for dilution. More diluted solutions were prepared daily from the stock solution. All other reagent grade chemicals were used without further purification.

Electrochemical measurements were performed with a home-made potentiostat/galvanostat. A three-electrode configuration was used for measurements, which consists of GCE working electrode, calomel (saturated) reference electrode and Pt counter electrode.

Scanning electron microscopy (SEM) images were obtained with a Hitachi S-4800 instrument at acceleration voltage of 15-20 kV and a working distance of 4-5 mm.

Atomic absorption spectrometry (AAS) model 3300 (Perkin-Elmer) was also used for determination of Hg<sup>2+</sup>.

**Pretreatment of GCE:** The GCE was prepared by cutting available plate-shaped glassy carbon (Tokai GC-20 company, NY) into cylinder-shape and mounting into Teflon tubes holder so that only a circular area of 0.071 cm<sup>2</sup> was exposed to the electrolyte. Glassy carbon electrode was polished with emery paper. Upon polishing, GCE was rinsed and ultra sonicated in distilled water for 3 min, rinsed and dried in air. Glassy carbon electrode was then electrochemically pretreated. Four methods were used for comparison, namely M1 to M4, as follows: M1: GCE was anodically polarized at potential of + 0.8 V for 300 s in 0.5 M H<sub>2</sub>SO<sub>4</sub> solution. M2: GCE was anodically polarized at + 0.8 V for 300 s followed by cathodic polarization at -1.0 V for 300 s in 0.5 M H<sub>2</sub>SO<sub>4</sub> solution. M3: GCE was cathodically polarized at - 1.0 V for 300 s, subsequently by anodic polarization at + 0.8 V for 300 s in 0.5 M H<sub>2</sub>SO<sub>4</sub> solution. M4: GCE was cathodically polarized at -1.0 V in 0.5 M H<sub>2</sub>SO<sub>4</sub> solution

for activation for various times from 30-300 s under stirring to study the influence of pretreatment time on the analyte signal of Hg<sup>2+</sup>. Glassy carbon electrode was then washed with distilled water and dried in air before electrodeposition of Au-NPs.

**Preparation of Au-NPs and PET-SAM:** Electrochemical deposition of Au-NPs on the GCE surface was carried out at potential of + 0.5 V in 1.0 × 10<sup>-3</sup> M HAuCl<sub>4</sub> solution for 600 s under stirring rate of 50 rpm. Au-NPs were deposited on GCE pretreated by methods M1 to M4, namely Au-NPs/GCE/M1 to M4.

Coating of PET-SAM onto Au-NPs electrodeposited on GCE (PET-SAM/Au-NPs/GCE) was prepared in 1.0 × 10<sup>-6</sup> M ethanolic solution of PET for 3 h at room temperature.

**Electrochemical measurements:** The formation of PET-SAM/GCE was investigated by cyclic voltammetry (CV) for reductive desorption. Measurement was performed in 0.5 M KOH solution, from 0.0 V to - 1.1 V at scan rate of 0.1 V s<sup>-1</sup>.

Redox behaviour of Au(III) in solution was studied by CV from 0.0 V to + 1.7 V at scan rate of 0.1 V s<sup>-1</sup> in 0.5 M H<sub>2</sub>SO<sub>4</sub> solution.

Determination of Hg<sup>2+</sup> was performed with two steps. First, Hg<sup>2+</sup> was chemically pre-concentrated by immersing PET-SAM/Au-NPs/GCE in a 0.1 M KCl + HCl solution, pH 6.7, containing Hg<sup>2+</sup> for a desired time under open circuit potential. During the preconcentration, the solution was efficiently stirred at 60 rpm. Second, reduction of Hg<sup>2+</sup> accumulated onto PET-SAM/Au-NPs/GCE was performed by differential pulse voltammetry (DPV). The voltammogram was recorded in a 0.1 M KCl + HCl solution, pH 3.0; the potential was scanned from + 0.7 V to + 0.3 V with pulse amplitude 0.050 V; pulse time 0.040 s; voltage step 0.005 V; step time 0.08 s; sweep rate 0.05 V s<sup>-1</sup>. All measurements were performed at room temperature.

**Real samples:** Ground water and seawater samples were collected in Quang Ninh and Da Nang beaches (Viet Nam). Samples were contained in polyethylene bottles and acidified at the sampling sites with 1.6 × 10<sup>-3</sup> M HNO<sub>3</sub>. Samples were stored in the laboratory at 4 °C. Samples used for AAS measurement were prepared by the procedure reported in elsewhere<sup>35</sup>.

## RESULTS AND DISCUSSION

**Effect of pretreatment methods on the surface morphology of Au-NPs/GCE:** In this section, we show the role of pretreatment methods in creating different surface morphologies of Au-NPs electrodeposited on GCE surface. Though electrodeposition of Au-NPs on the GCE surface was reported elsewhere<sup>36</sup>, but we attempted investigation for selecting a suitable electrodeposition potential for our electrochemical cell. Since the appearance of a reduction peak at + 0.58 V in the voltammogram obtained for reduction of solution bound Au(III) to Au(0), a potential of + 0.50 V was chosen to electrodeposit Au-NPs on the GCE surface. This result is analogous with that has been reported in the literature<sup>36</sup>. The surface morphology of Au-NPs/GCE obtained by methods M1 to M4 was imaged by SEM and shown in Fig. 1. It can be seen that the arrangement of Au-NPs pretreated by methods M2 and M4 (Fig. 1b and 1d) is better ordered than that pretreated

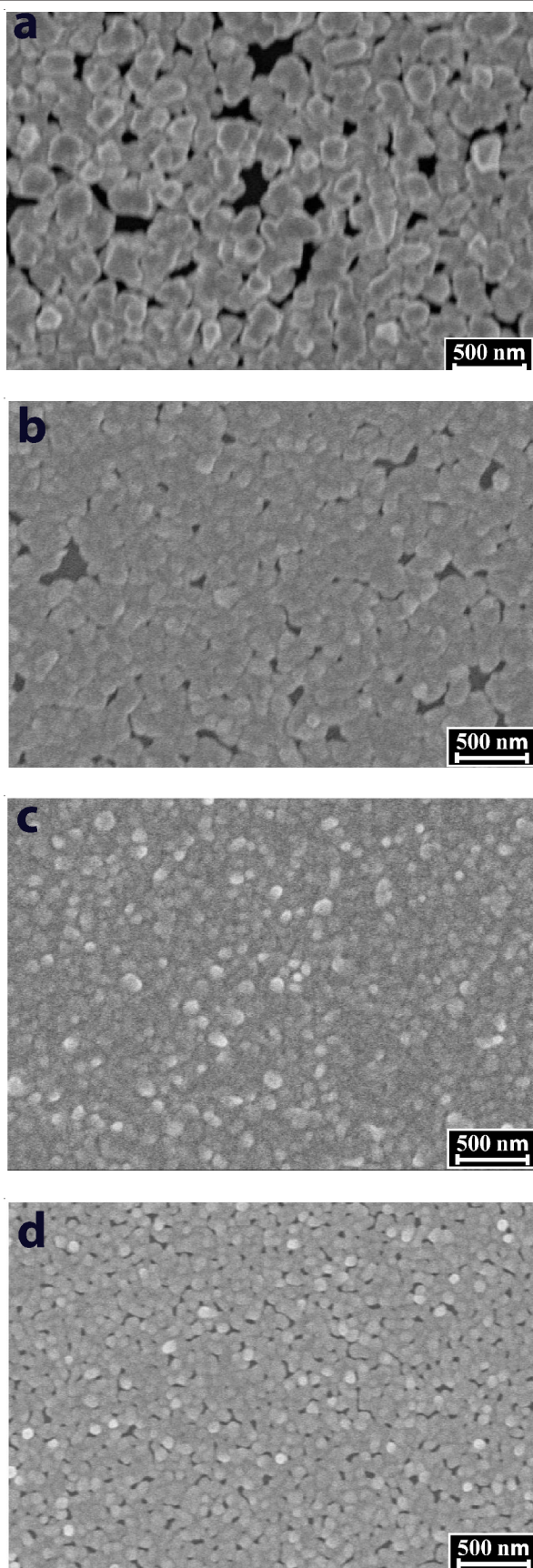


Fig. 1. SEM images of Au-NPs/GCE pretreated by different methods: (a) M1; (b) M2; (c) M3; (d) M4

by methods M1 and M3 as their disorder significantly increase, yielding the roughness in the nanometer level (Fig. 1a and

1c). Keep in mind that the final polarization step in methods M2 and M3 is similar with M4 and M1, respectively. Therefore, SEM images indicate that the roughness of Au-NPs/GCE depends on the direction of polarization (M1, M4) as well as on the order of polarization steps (M2, M3). These obtained results are consistent with those obtained by Denkansri *et al.*<sup>37</sup> by scanning tunneling microscopy technique for imaging the change in morphology and structure of the GCE surface pretreated by different methods. Authors concluded that anodic polarization has a main part in getting a rough surface as a consequence of the oxidation process. It is relevant to the oxygen-carbon functional groups created on the surface due to the electrochemical polarization, Laser and Ariel reported that anodic polarization can form oxygen-containing functional groups, such as carbonyl or carboxyl that subsequently can be reduced to hydroxyl groups at more negative potential<sup>38</sup>. Meanwhile, Hangovan *et al.*<sup>39</sup> proved that the exclusive reduction polarization reveals creation of >C-O-. Hence, we attribute that the reason for getting the difference in arrangement of Au-NPs is the formation of functional groups created by electrochemical processes that could promote or eliminate the ordered of graphite particles on the GCE surface. Thus, the reversibility of the order of anodic and cathodic polarizations can influence the formation of functional groups in the final step, leading to the change in arrangement of Au-NPs on the GCE surface due to the change of the structure of the active layer.

Furthermore, one can be clearly seen the variation in size of gold particles caused by pretreatment methods. The average size in diameter of Au-NPs was estimated for M1 to be 220, M2 175, M3 110 and M4 70 nm. This variation indicates that the cathodic polarization and its order in the final step can also reduce the size of Au-NPs/GCE. Shi *et al.*<sup>40</sup> reported that potentiostatic activation by anodic polarization can corrode graphitic particles to create void space in the interior of the activated film. We attribute, therefore, that the anodic polarization step in methods M1 to M3 causes an increase in the size of Au-NPs because such void space in the active film is probably essential for the growth of gold particles in the neighbour sites. In addition, the order of polarization steps can also influence the size of particles, that can be elucidated by the oxygen-containing surface functional groups formed by cathodic polarization are not completely oxidized in the subsequent anodic polarization<sup>41</sup>. Therefore, for instant, if the cathodic polarization is initially carried out, it will reduce the corrosion of graphitic particles in the subsequent anodic polarization step, precluding the growth of gold particles.

**Optimization of factors for determination of  $Hg^{2+}$ :** Au-NPs/GCE are analogous to Au substrate for the strong chemical affinity between mercapto group and the gold surface that easily enables the formation of SAM of alkanethiols on Au<sup>42,43</sup>. In our study, PET-SAM was selected for coating the Au-NPs/GCE because it enables to have coordination with  $Hg^{2+}$  via N-donor of pyridine. The formation of the PET-SAM on Au-NPs was examined by CV in 0.5 M KOH solution. A reductive desorption peak appeared at -0.85 V on the voltammogram indicates the presence of PET SAM on Au-NPs/GCE<sup>44</sup>. However, the difference in morphology of Au-NPs can influence the assembly of PET molecules, leading to the effects on the

coordination with  $\text{Hg}^{2+}$ . We, thus, employed directly the term of peak current ( $i_{p\text{Hg}^{2+}}$ ) obtained from differential pulse voltammogram for reduction of  $\text{Hg}^{2+}$  bound to the PET-SAM *via* pre-concentration to evaluate the appropriateness of the surface morphologies of Au-NPs. The voltammograms for such reduction of  $\text{Hg}^{2+}$  are depicted in the inset of Fig. 2. As seen, when Au-NPs/GCE is coated with PET-SAM, curves show only a peak at potential of + 0.53 V. When  $\text{Hg}^{2+}$  is pre-concentrated onto the Au-NPs/GCE without coating PET-SAM, the curve becomes flat as typically shown for Au-NPs/GCE/M4. These results clearly indicate the role of PET-SAM in the pre-concentration for accumulation of  $\text{Hg}^{2+}$ .

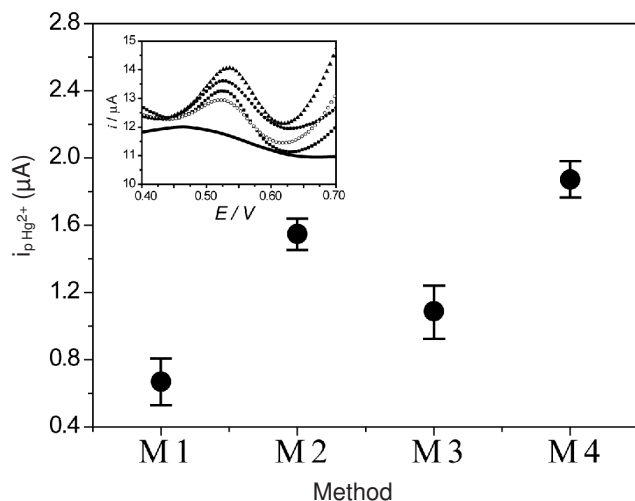


Fig. 2. Dependence of the peak current obtained from the differential pulse voltammograms for reduction of  $\text{Hg}^{2+}$  bound to PET-SAM/Au-NPs/GCE on different pretreatment methods. Inset: differential pulse voltammograms for reduction of  $\text{Hg}^{2+}$  bound to PET-SAM/Au-NPs/GCE pretreated by methods M1 (■); M2 (●); M3 (○); M4 (▲), recorded in 0.1 M KCl + HCl solution, pH = 3.0. Pre-concentration was carried out in 0.1 M KCl + HCl, pH = 6.7 solution containing  $5.0 \times 10^{-9}$  M  $\text{Hg}^{2+}$  for all methods

The variation of  $i_{p\text{Hg}^{2+}}$  obtained by pretreatment methods is shown in Fig. 2. It can be clearly seen that the value of  $i_{p\text{Hg}^{2+}}$  obtained by methods M1 and M3 are significantly lower than that obtained by methods M2 and M4. The value of  $i_{p\text{Hg}^{2+}}$  reaches the maximum when the GCE surface is pretreated by method M4. These results clearly indicate the advantage of method M4 compared with the others in enhancing the sensitivity for detection of  $\text{Hg}^{2+}$ . Such increase in  $i_{p\text{Hg}^{2+}}$  should be relevant to the morphology of Au-NPs because it affects the formation of PET-SAM. As presented, the decrease in size of gold particles obtained by method M4 increases the microscopic area of gold surface, meanwhile their order can improve closed-packed monolayer. These characters are essential for increasing the amount of PET molecules assembled on Au-NPs/GCE. This was also examined as the charge estimated from the area under the peak for reductive desorption of PET-SAM formed on Au-NPs/GCE/M4 was greater than that formed on Au-NPs/GCE/M1 to M3. Since the advantage of M4, this method was selected to activate GCE use for further studies.

Particularly, experimental conditions used in M4 were optimized with the indication of  $i_{p\text{Hg}^{2+}}$  as shown in Fig. 3. The

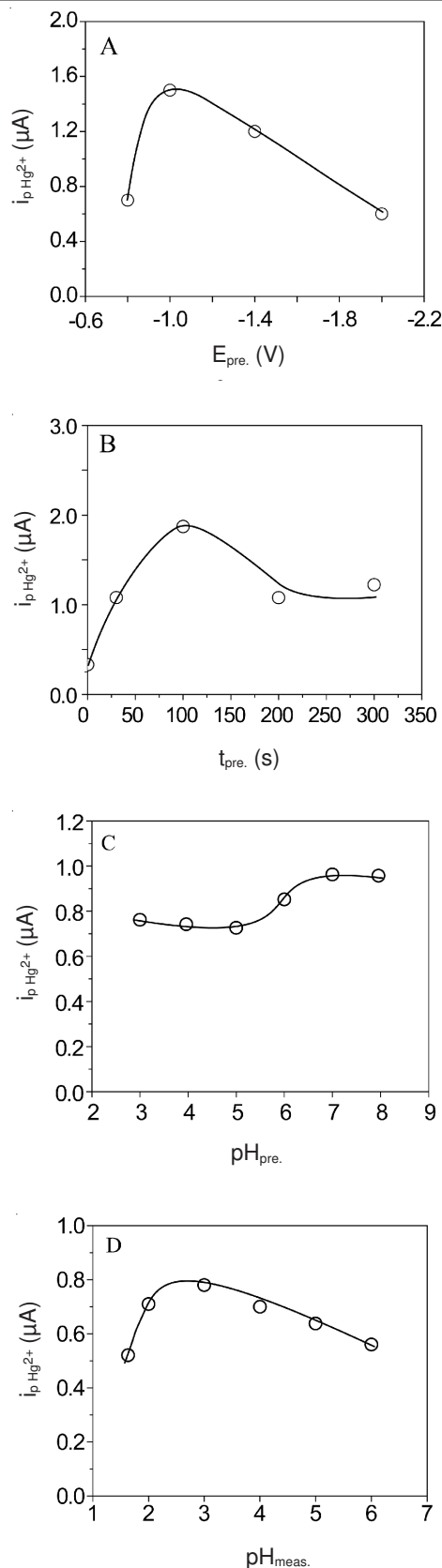


Fig. 3. Dependence of the peak current obtained from the differential pulse voltammograms for reduction of  $\text{Hg}^{2+}$  bound to PET-SAM/Au-NPs/GCE on: the cathodic polarized potential for pretreatment of GCE (A); pretreatment time (B) in 0.5 M  $\text{H}_2\text{SO}_4$  solution and pH of solutions used for pre-concentration of  $\text{Hg}^{2+}$  (C); for DPV measurement (D). Pre-concentration was performed in 0.1 M KCl + HCl, pH = 6.7 containing  $5.0 \times 10^{-9}$  M  $\text{Hg}^{2+}$  for all measurements

dependence of  $i_{\text{pHg}^{2+}}$  on the cathodic potentials used for GCE pretreatment ( $E_{\text{pre}}$ ) is depicted in Fig. 3a. As seen, the optimized  $E_{\text{pre}}$  corresponding to the maximum value of  $i_{\text{pHg}^{2+}}$  can be achieved at potential of -1.0 V and significantly reduce with increasing  $E_{\text{pre}}$  to the negative direction. Such variation of  $i_{\text{pHg}^{2+}}$  reflects the influence of the cathodically polarized potential on the formation of PET-SAM. We attribute that exceedingly negative potential applied to GCE is related to the change in structure of the activated layer on the GCE surface that can affect subsequently the morphology of Au-NPs. We attempted to take SEM images, however, obtained results could not reflect clearly any changes of the active layer. It may be attributed to the change in nanometer level that could not be detected by SEM. Though, such change in the structure is consistent with the significant decrease of  $i_{\text{pHg}^{2+}}$  as the polarization time ( $t_{\text{pre}}$ ) exceeds 100 s as shown in Fig. 3b.

The dependence of  $i_{\text{pHg}^{2+}}$  on the pH of solutions was also investigated as shown in Fig. 3C and 3D. It is observed that  $i_{\text{pHg}^{2+}}$  approached the maximum value at pH 6.7 of the solution used for preconcentration of  $\text{Hg}^{2+}$  ( $\text{pH}_{\text{pre}}$ ) and pH 3.0 of the solution used for DPV measurement ( $\text{pH}_{\text{meas}}$ ). The difference in pH of these solutions suggests that deprotonation and protonation of N in pyridine facilitates the binding with  $\text{Hg}^{2+}$  and reduction of  $\text{Hg}^{2+}$  bound to PET-SAM, respectively. This is similar with the formation of covalent Hg-N bonds that has been reported in literature as the formation of  $\text{Hg}^{2+}$ -thiamine in DNA was studied<sup>45-47</sup>. According to these studies, thiamine residues bind to  $\text{Hg}^{2+}$  with the ratio of 2:1, accompanied with the release of protons from thiamine. In the present work, the reduction of  $\text{Hg}^{2+}$  bound to PET-SAM was studied by CV in 0.1 M KCl + HCl solution, pH 3.0, for PET-SAM/Au-NPs/GCE preconcentrated with  $5.0 \times 10^{-9}$  M  $\text{Hg}^{2+}$ . The obtained voltammogram showed reversible redox waves with peak-to-peak separation ( $\Delta E_{\text{p}}$ ) value was *ca.* 60 mV, suggesting rapid  $1 e^-$  electron transfer reaction kinetic. Since, when the reduction of  $\text{Hg}^{2+}$  bound to PET SAM takes place, one of two N-donor bound to  $\text{Hg}^{2+}$  is released and protonated for stabilization. This result is consistent with the case of electrochemical reduction of  $\text{Hg}^{2+}$  bound to 1,4-benzenedimethanethiol (BDMT) monolayer assembled on a Au electrode yields  $\text{Hg}^+$ -BDMT and subsequently to  $\text{Hg}^0$ -BDMT at  $E^0$  of +0.48 and +0.2 V, respectively<sup>48</sup>.

The duration of preconcentration in solution containing  $\text{Hg}^{2+}$  was also investigated thorough the evaluation of  $i_{\text{pHg}^{2+}}$ . The dependence of  $i_{\text{pHg}^{2+}}$  on the preconcentration time ( $t_{\text{Hg}^{2+}}$ ) with the presence of  $\text{Hg}^{2+}$  in various concentrations is shown in Fig. 4. As seen, the variation of  $i_{\text{pHg}^{2+}}$  by  $t_{\text{Hg}^{2+}}$  was distinct in two different ranges of the concentration of  $\text{Hg}^{2+}$ . In the low concentration range, below  $5.0 \times 10^{-9}$  M,  $i_{\text{pHg}^{2+}}$  gradually increased with increasing  $t_{\text{Hg}^{2+}}$  within 80 min and then approached to the constancy. Such variation suggests the formation of a monolayer of  $\text{Hg}^{2+}$  on the PET SAM. Whilst in the high concentration range, greater than  $1.5 \times 10^{-8}$  M,  $i_{\text{pHg}^{2+}}$  increased considerably and started approaching to the constancy within only around 10 min (the exact inflection time depends on the concentration of  $\text{Hg}^{2+}$ ). After this duration of time the variation of  $i_{\text{pHg}^{2+}}$  became linear with increasing  $t_{\text{Hg}^{2+}}$ , indicating that the preconcentration in this step was a kinetic process and driven by the formation of multilayers of  $\text{Hg}^{2+}$ .

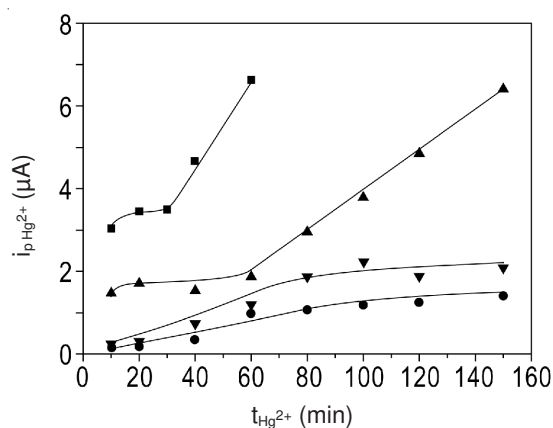


Fig. 4. Dependence of the peak current obtained from the differential pulse voltammograms for reduction of  $\text{Hg}^{2+}$  bound to PET-SAM/Au-NPs/GCE on the pre-concentration time in 0.1 M KCl + HCl, pH = 6.7 solution containing  $\text{Hg}^{2+}$  at different concentrations:  $2.5 \times 10^{-9}$  M (●);  $5.0 \times 10^{-9}$  M (▼);  $2.5 \times 10^{-8}$  M (▲),  $1.0 \times 10^{-7}$  M (■)

Taking into account these variations of  $i_{\text{pHg}^{2+}}$ , pre-concentration time of 20 and 80 min were chosen for the high and low concentration ranges, respectively. Though the duration of preconcentration for the case of low concentration range is not too short, but the high sensitivity and wide linear range make the PET-SAM/Au-NPs/GCE become essential for study as presented as following.

**Use of PET-SAM/Au-NPs/GCE for determination of  $\text{Hg}^{2+}$  at trace concentrations:** Fig. 5 exhibits differential pulse voltammograms for reduction of  $\text{Hg}^{2+}$  bound to PET-SAM/Au-NPs/GCE/M4 preconcentrated from solutions containing various concentrations of  $\text{Hg}^{2+}$ . As seen, the voltammograms show the increase in the height of a well-defined peak at potential of +0.53 V as increasing the concentration of  $\text{Hg}^{2+}$ . This clearly indicates that the peak corresponds to the reduction of  $\text{Hg}^{2+}$  bound to the PET-SAM. The dependence of the  $i_{\text{pHg}^{2+}}$  versus the concentration of  $\text{Hg}^{2+}$  in solution is depicted in the insets of Fig. 5. The calibration curve consists of two linear regions corresponding to the low and high concentration ranges. The first region demonstrates linearity over concentration range of  $5.0 \times 10^{-11}$  to  $5.0 \times 10^{-9}$  M. The second linear range is from  $5.0 \times 10^{-9}$  to  $7.0 \times 10^{-7}$  M. The relative equation for each range is  $i_{\text{pHg}^{2+}} (\mu\text{A}) = 0.3602 \times C + 0.1127$  with correlation coefficient ( $R^2$ ) = 0.993 and  $i_{\text{pHg}^{2+}} (\mu\text{A}) = 0.1073 \times C + 0.7877$ ,  $R^2 = 0.998$ , respectively. The detection limit approached  $4.5 \times 10^{-12}$  M, as estimated from three times the standard deviation of the background noise according to the IUPAC recommendation. This value is well below the detection limit that was reported previously. In these studies, the modification of GCE with Au-NPs<sup>49</sup>, gold electrodes with SAM<sup>19,21,24,50</sup> or gold micro/nanopore arrays with SAM<sup>51</sup> has been used.

The repeatability of the response of  $5.0 \times 10^{-10}$  M  $\text{Hg}^{2+}$  was evaluated with six replicates on five different electrodes. The relative standard deviation was 2.7 %. This value can be considered satisfactory, taking into account the relatively ultra low concentration level involved.

The stability of the PET-SAM/Au-NPs/GCE/M4 was studied by potential cycling as the potential was scanned between +0.7 and +0.3 V with scan rate of 0.1 V/s in 0.1 M KCl + HCl solution, pH = 3.0. After that, the modified GCE

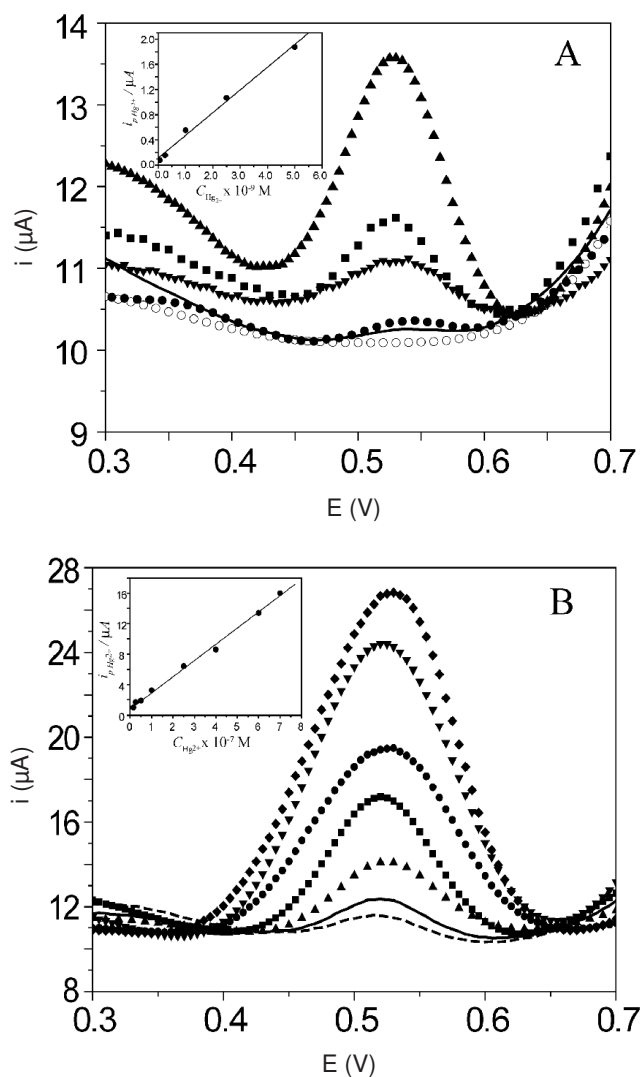


Fig. 5. Differential pulse voltammograms for reduction of  $\text{Hg}^{2+}$  bound to PET-SAM/Au-NPs/GCE/M4 pre-concentrated in different concentrations of  $\text{Hg}^{2+}$ . Fig. 5A: background (●);  $5.0 \times 10^{-11}$  (thin line);  $2.5 \times 10^{-10}$  (▼);  $1.0 \times 10^{-9}$  (■);  $2.5 \times 10^{-9}$  (▲);  $5.0 \times 10^{-9}$  M (▲) by pre-concentration time of 80 min. Fig. 5B:  $1.5 \times 10^{-8}$  (dotted line);  $2.5 \times 10^{-8}$  (thin line);  $1.0 \times 10^{-7}$  (▲);  $2.5 \times 10^{-7}$  (■);  $4.0 \times 10^{-7}$  (●);  $6.0 \times 10^{-7}$  (▼);  $7.0 \times 10^{-7}$  M (◆) by pre-concentration time of 20 min. Voltammograms were recorded in 0.1 M KCl + HCl solution, pH = 3.0. Insets: corresponding calibration curves for determination of  $\text{Hg}^{2+}$  by PET-SAM/Au-NPs/GCE/M4

was used again for preconcentration in solution containing  $5.0 \times 10^{-10}$  M  $\text{Hg}^{2+}$  and followed by DPV measurement. It is noticeable that the PET-SAM was stable for more than 10 potential cycles with  $i_{\text{pHg}^{2+}}$  was considered as an indication for the stability of the modified electrode.

The selectivity of the PET-SAM/Au-NPs/GCE/M4 for  $\text{Hg}^{2+}$  was also evaluated with the term of  $i_{\text{pHg}^{2+}}$  in the presence of some possible interfering foreign cations that were intentionally introduced into the solution containing  $\text{Hg}^{2+}$  during preconcentration. Foreign cations employed in our study were  $\text{Zn}^{2+}$ ,  $\text{Cd}^{2+}$ ,  $\text{Pb}^{2+}$ ,  $\text{Cu}^{2+}$ ,  $\text{Cr}^{3+}$ ,  $\text{Ni}^{2+}$ ,  $\text{Bi}^{2+}$ ,  $\text{Mn}^{2+}$ ,  $\text{Fe}^{2+}$ ,  $\text{Fe}^{3+}$ . These cations were chosen because they possibly coexist with  $\text{Hg}^{2+}$ . With the presence of these foreign cations in solution, the potential of the reduction peak of  $\text{Hg}^{2+}$  on voltammogram was not varied, as shown in the inset of Fig. 6. This suggests the

insignificant interference from foreign cations to the reduction of  $\text{Hg}^{2+}$ . The selectivity of the PET-SAM/Au-NPs/GCE/M4 to  $\text{Hg}^{2+}$  in the preconcentration step was evaluated by calculating the ratio ( $i_{\text{pHg}^{2+}}^{\text{P}}/i_{\text{pHg}^{2+}}^{\text{0}}$ ), where  $i_{\text{pHg}^{2+}}^{\text{P}}$  and  $i_{\text{pHg}^{2+}}^{\text{0}}$  are the current of the peak at potential of + 0.53 V on the differential pulse voltammograms in the presence and absence of the foreign cations, respectively. The dependence of the ratio ( $i_{\text{pHg}^{2+}}^{\text{P}}/i_{\text{pHg}^{2+}}^{\text{0}}$ ) on the concentration of  $\text{Hg}^{2+}$  with the presence of the foreign cations in different concentrations is shown in Fig. 6. It can be clearly seen that a 100-fold excess of the foreign cations hardly causes a significant change of the peak current for reduction of  $\text{Hg}^{2+}$ . However, the presence of a 200-fold excess of the foreign cations could interfere the peak current. The value  $i_{\text{pHg}^{2+}}^{\text{P}}$  could be reduced to 50 % at the concentration of  $\text{Hg}^{2+}$  of  $5.0 \times 10^{-10}$  M. But in practice, a hundred-fold excess is tolerable for analysis of samples having very low concentration of  $\text{Hg}^{2+}$ .

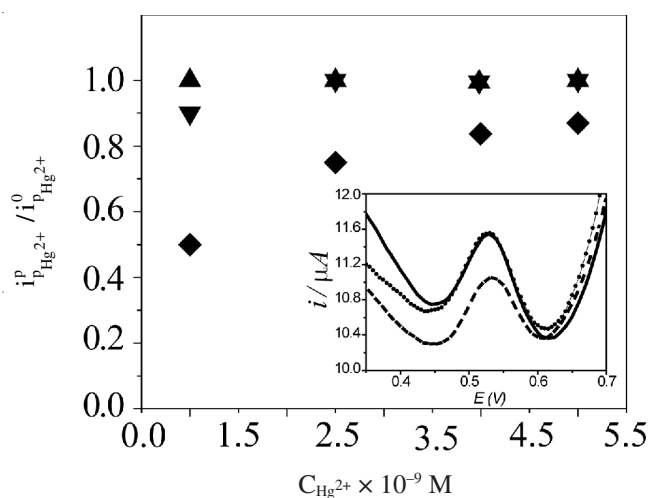


Fig. 6. Dependence of the normalized peak current obtained from the differential pulse voltammograms for reduction of  $\text{Hg}^{2+}$  bound to PET-SAM/Au-NPs/GCE on the concentration of  $\text{Hg}^{2+}$  in the absence (▲) and the presence of foreign cations at concentrations:  $1.0 \times 10^{-7}$  M (▼);  $2.0 \times 10^{-7}$  M (◆)

In order to evaluate the applicability in determination of the trace concentration of  $\text{Hg}^{2+}$  in real samples, the PET-SAM/Au-NPs/GCE/M4 was employed for analyzing  $\text{Hg}^{2+}$  in ground water and sea water.  $\text{Hg}^{2+}$  was quantified by the external calibration curve method. Samples were also analyzed using AAS for comparison. The repeatability of the analysis using the modified GCE was illustrated by the precision obtained for a series of five repetitions ( $n = 5$ ). The results of the analysis of  $\text{Hg}^{2+}$  are summarized in Table-1, reflecting a good agreement between two methods. Thus, the analysis of real samples shows that PET-SAM/Au-NPs/GCE/M4 is sufficiently sensitive to allow the determination of  $\text{Hg}^{2+}$  in the trace concentration in natural water.

## Conclusion

Use of the exclusively cathodic polarization method to pretreat GCE for electrochemical deposition of Au-NPs and followed by coating with PET SAM on the surface has exhibited the advantage in enhancing the sensitivity of determination of  $\text{Hg}^{2+}$ . Use of this simple pretreatment method decreases the size of gold particles and their disordered arrangement

TABLE-1  
DETERMINATION OF Hg<sup>2+</sup> IN WATER SAMPLES  
USING PET-SAM/Au-NPs/GCE AND AAS METHOD

Samples	Concentration of Hg <sup>2+</sup> determined by methods		
	PET/GNPs/GCE (× 10 <sup>-10</sup> M)	AAS (× 10 <sup>-10</sup> M)	Relative deviation (%)
Ground water	7.0 ± 0.040 <sup>a</sup>	6.1 ± 1.640	14.7
Sea water <sup>1</sup>	7.1 ± 0.047 <sup>a</sup>	5.7 ± 2.060	25.4
Sea water <sup>2</sup>	12.2 ± 0.031 <sup>a</sup>	11.1 ± 1.150	9.9

<sup>a</sup>Data are presented as mean ± SD. <sup>1</sup>Sea water sample in Quang Ninh beach. <sup>2</sup>Sea water sample in Da Nang beach.

compared with the ones included both anodic and cathodic polarizations or exclusive anodic polarization. These characters are attributed to be the reasons for increasing in the peak current on the differential pulse voltammogram for determination of Hg<sup>2+</sup>.

### ACKNOWLEDGEMENTS

This research is funded by Viet Nam National Foundation for Science and Technology Development (NAFOSTED) under grant number 104.03.125.09.

### REFERENCES

- J.F. Risher and S.N. Amler, *Neuro Toxicol.*, **26**, 691 (2005).
- A.K. Das, M.de la Guardia and M.L. Cervara, *Talanta*, **55**, 1 (2001).
- J.M. Ombaba, *Microchem. J.*, **53**, 195 (1996).
- H. Bagheri and A. Gholami, *Talanta*, **55**, 1141 (2001).
- H.E.L. Armstrong, W.T. Corns, P.B. Stockwell, G. O'Connor, L. Ebdon and E.H. Evans, *Anal. Chim. Acta*, **390**, 245 (1999).
- A.C. Barbosa and G.A. East, *Ecol. Trace Elem. Res.*, **60**, 153 (1997).
- L.N. Suvarapu, Y.-K. Seo and S.-O. Baek, *Asian J. Chem.*, **25**, 5599 (2013).
- N. Yu. Stojko, Kh.Z. Brainina, C. Faller and G. Henze, *Anal. Chim. Acta*, **371**, 145 (1998).
- O. Abollino, A. Giacomino, M. Malandrino, S. Marro and E. Mentasti, *J. Appl. Electrochem.*, **39**, 2209 (2009).
- F. Okçu, F. Ertas, H.I. Gökçel and H. Tural, *Turk. J. Chem.*, **29**, 355 (2005).
- E.P. Gil and P. Ostapczuk, *Anal. Chim. Acta*, **293**, 55 (1994).
- Z. Gao, P. Li and Z. Zhao, *Microchem. J.*, **43**, 132 (1991).
- N.L.D. Filho, D.R. Carmo, L. Caetano and A.H. Rosa, *Anal. Sci.*, **21**, 1359 (2005).
- L.M. Aleixo, M. de F.B. Souza, O.E.S. Godinho, G.de O. Neto and Y. Gushikem, *Anal. Chim. Acta*, **271**, 143 (1993).
- S. Güney, G. Yildiz and G. Yapar, *Int. J. Electrochem.*, Article ID 529415 (2011).
- K.-S. Yoo, S.-B. Woo and J.-Y. Jyoung, *Bull. Korean Chem. Soc.*, **24**, 27 (2003).
- H. Ju and D. Leech, *J. Electroanal. Chem.*, **484**, 150 (2000).
- E.-R.E. Mojica and F.E. Merca, *J. Appl. Sci.*, **5**, 1461 (2005).
- N. Daud, N.A. Yusof and T.W. Tee, *Int. J. Electrochem. Sci.*, **6**, 2798 (2011).
- S. Huan, C. Jiao, Q. Shen, J. Jiang, G.M. Zheng, G.H. Huang, G.L. Shen and R.Q. Yu, *Electrochim. Acta*, **49**, 4273 (2004).
- S. Berchmans, S. Arivukkodi and V. Yegnaraman, *Electrochem. Commun.*, **2**, 226 (2000).
- D. Han, Y.-Rae Kim, J.W. Oh, T.H. Kim and R.K. Mahajan, *Analyst.*, **134**, 1857 (2009).
- A.M. Etorki, E. Elakkari and E. Ali, *Chem. Sen.*, **1**, 10 (2011).
- D. Wu, Q. Zhang, X. Chu, H. Wang, G. Shen and R. Yu, *Biosens. Bioelectron.*, **25**, 1025 (2010).
- T. Hezard, K. Fajerweg, D. Evrard, V. Collière, P. Behra and P. Gros, *J. Electroanal. Chem.*, **664**, 46 (2012).
- J.C. Love, L.A. Estroff, J.K. Kriebel, R.G. Nuzzo and G.M. Whitesides, *Chem. Rev.*, **105**, 1103 (2005).
- H. Zhang and L.A. Coury, *Anal. Chem.*, **65**, 1552 (1993).
- R.C. Engstrom, *Anal. Chem.*, **54**, 2310 (1982).
- N. Cenas, J. Rozgaite, A. Pocius and J. Kulys, *J. Electroanal. Chem.*, **154**, 121 (1983).
- M. Gross and J. Jordan, *Pure Appl. Chem.*, **56**, 1095 (1984).
- R.L. McCreery, In ed.: A.J. Bard, Carbon Electrode: Structural Effects on Electron Transfer Kinetics, Electroanalytical Chemistry, Dekker New York, Vol. 17, pp. 221-374 (1991).
- T. Nagaoka and T. Yoshino, *Anal. Chem.*, **58**, 1037 (1986).
- M.S. El-Deab, T. Sotomura, T. Okajima and T. Ohsaka, *J. Electroanal. Chem.*, **152**, C730 (2005).
- H.S. Wang, H.X. Ju and H.Y. Chen, *Electroanalysis*, **13**, 1105 (2001).
- K.S. Lee, H.S. Choi, S.T. Kim and Y.S. Kim, *J. Korean Chem. Soc.*, **4**, 35 (1991).
- M.O. Finot, G.D. Braybrook and M.T. Mc Dermott, *J. Electroanal. Chem.*, **466**, 234 (1999).
- A. Denkansi, J. Stevanovic, R. Stevanovic, B.Z. Nikolic and V.M. Jovanovic, *Carbon*, **39**, 1195 (2001).
- D. Laser and M. Ariel, *J. Electroanal. Chem.*, **52**, 291 (1974).
- G. Hangovan and K.C. Pillai, *J. Solid State Electrochem.*, **3**, 357 (1999).
- K. Shi and K.-K. Shiu, *Anal. Chem.*, **74**, 879 (2002).
- M. Noel and P.N. Anantharaman, *Surf. Coatings Technol.*, **28**, 161 (1986).
- M.D. Porter, T.B. Bright, D.L. Allara and C.E.D. Chidsey, *J. Am. Chem. Soc.*, **109**, 3559 (1987).
- R.G. Nuzzo and D.L. Allara, *J. Am. Chem. Soc.*, **105**, 4481 (1983).
- C.A. Widrig, C. Chung and M.D. Porter, *J. Electroanal. Chem.*, **310**, 335 (1991).
- T. Yamane and N. Davidson, *J. Am. Chem. Soc.*, **83**, 2599 (1961).
- S. Katz, *Biochim. Biophys. Acta*, **68**, 240 (1963).
- Y. Miyake, H. Togashi, M. Tashiro, H. Yamaguchi, S. Oda, M. Kudo, Y. Tanaka, Y. Kondo, R. Sawa, T. Fujimoto, T. Machinami and A. Ono, *J. Am. Chem. Soc.*, **128**, 2172 (2006).
- M. Riskin, B. Basnar, E. Katz and I. Willner, *Chem. Eur. J.*, **12**, 8549 (2006).
- O. Abollino, A. Giacomino, M. Malandrino, G. Piscionieri and E. Mentasti, *Electroanalysis*, **20**, 75 (2008).
- Z. Cao, S. Long, X. Shi, J.L. Zeng, L.X. Sun and R.H. Yang, *Appl. Mech. Mater.*, **44-47**, 2553 (2011).
- X.C. Fu, X. Chen, Z. Guo, L.T. Kong, J. Wang, J.H. Liu and X.J. Huang, *Electrochim. Acta*, **56**, 463 (2010).